

2D Seismic Interpretation to Understand the Structural Geometry of Cretaceous Sand Packages, Jabo Field, Pakistan

M.J. Khan*, M. Umar, M. Khan and A. Das

Department of Earth and Environmental Sciences, Bahria University (Karachi Campus), Karachi, Pakistan

ARTICLE INFO

Article history:

Received: 14 January, 2019

Accepted: 19 December, 2019

Published: 30 December, 2019

Keywords:

Seismic interpretation,
Jabo field,
Badin rift basin,
Hydrocarbons,
Southern Sindh monocline

ABSTRACT

This study is focused on interpretation of 2D seismic reflection profiles coupled with borehole logs of Jabo Field (JF). The seismic interpretation revealed the configuration of basin fill deposits, subsurface geological structural geometries and their association with tectonic interventions in JF, Lower Indus Basin, Pakistan. Primarily, the tectonic stresses control the dimensions, geometry and style of deformation of geological structures which contribute in development of hydrocarbon trapping system. We have studied the structural geometries of Cretaceous sand packages which serve as a reservoir in oil & gas prone JF. Isochron and isopach maps were prepared to delineate the geological structure of Top of Lower Goru (TLG), Top of Middle Sand (TMDS) and Top of Basal Sand (TBSL). TLG forms a three-way dip closure bounded by a NE-SW trending major fault of the JF; the geological structure at TMDS level is a two-way fault bounded since to the north and south it is bounded by dipping blocks; and the structural closure at TBSL level is two-way dip and two-way faults bounded. The structural closure to the north and south provided by the dipping horizons, from west by Main Fault Line (MFL) of JF and from east the closure is provided both by Secondary Fault Line (SFL) of the JF and dipping surfaces of sand packages. Interpretation shows the geological implications of extensional regime in the study area, dominated by horst and graben structures which are believed to be promising hydrocarbon traps.

1. Introduction

The seismic reflection profiles are resourceful dataset utilized to unearth the local structural geometries, intervention of tectonic stresses in geological times, the signatures of petroleum system elements, hydrocarbon traps; however, provide slight insight about the subsurface geological structures at regional scale. Generally, reflectors picking or horizon marking is carried out by inspecting seismic sections passing near to well, and are interpreted on the basis of dominant reflection coefficient. The geological structures (folds and faults) are significant traps in hydrocarbon exploration in offshore and onshore areas [1]. The interpretation of seismic sections primarily focused on the picking of the reflectors with a careful analysis of reflection configuration, reflection continuity and reflection amplitudes [2]. The interpretation of faults is also essential to reckon the fault components, structural style and hydrocarbon trap [3].

The Lower Goru sand sequences (Cretaceous age) host the hydrocarbons at several fields in Lower Indus Basin (LIB) that produce hydrocarbons from structural traps (typically fault closures); however, few stratigraphic traps are also producing in the Badin area [4]. The tectonic pulses attempts to implicate the brittle deformation and somehow controlled the dimensional geometries of geological structures. The seismic profiles helped to interpret the complex subsurface geological models subject to the tectonic and stratigraphic changes [5].

The Jabo Field (JF) is covering an area of 1265.3 km² which is a prolific field of southern Badin concession, having a potential of 5.69 million barrel oil production [6]. Badin

concession area has been well-explored by passive (aeromagnetic and gravity) and active (seismic reflection) geophysical methods [7]. A total of 119 exploratory wells have been drilled in the Badin blocks, in which there have been discoveries of 19 gas fields, 15 oil fields and 18 oil and gas fields [8, 9].

The stratigraphic configuration is similar in Badin concession area including the JF: the deepest Chiltan Limestone of Jurassic age overlain by the early Cretaceous marine sand-shale sequence of the Sembar and Goru formations [1, 9]. The Sembar formation (early Cretaceous) rich in organic shale which act as source rock of JF and LIB [10]. The Lower Goru formation is divided into predominant sand-shale packages; however, we emphasized on sand packages of Lower Goru and collectively named them as Cretaceous Sand Packages (CSP) in this study. These CSP act as reservoir in LIB charged by the underlying Sembar formation in the JF and capped by the overlying marl and claystone of Upper Goru [11].

The LIB has been deformed by three major tectonic episodes over the geological times (Cretaceous to Paleocene). (1) Prior to Early Cretaceous (Pre-Chiltan to Sembar), (2) Middle to late Cretaceous (Basal Sand to Upper Goru), and (3) Post Paleocene (uplift and doming) [12]. These three major episodes have been affected by the depositional environment, sedimentology and have impact on overall structural developments in the LIB [12, 13]. The Indian plate started separating away from the Madagascar about 130 million year ago and began moving northward and developed Sindh monocline [13, 14]. The northward drift of Indian plate

*Corresponding author: mjahangir.bukc@bahria.edu.pk

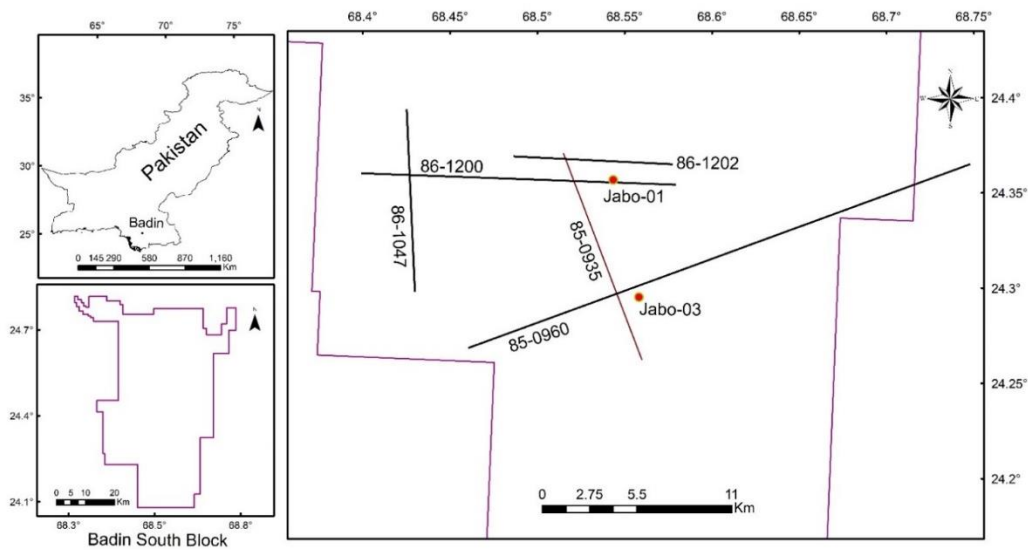


Fig. 1: The base map is showing study area, seismic lines and well data used in this study.

generated compression while accompanying anticlockwise rotation produced extensional stresses [14]. The extensional tectonic settings are ideal for the formation of main entrapment mechanism (horst and graben types structures) in southern Sindh monocline, Badin rift basin and JF [14]. The series of tilted horst and graben structures exist below the base of Paleocene unconformity [15] which were formed during the late Cretaceous times [16].

This study emphasizes on interpretation of horizons of CSP with integration of synthetic seismogram and borehole data to understand the structural style and its implications in trapping mechanism. The isochron and isopach maps of sand packages (top sands, middle sand and basal sand of Lower Goru) helped us to delineate the association of tectonic stresses and fault analysis at various levels through graphical modelling.

2. Methodology

We have utilized the seismic sections of 2D lines: PK 85-0960 (dip line), PK 85-0935 (strike line), PK 86-1200 (dip line), PK 86-1202 (strike line), PK86-1047 (strike line) coupled with substantial information of well logs of two boreholes Jabo-01 and Jabo-03. The seismic lines oriented along the East-West are dip lines whereas the strike lines are running from North to South (Fig. 1). The dataset was provided by the Directorate General of Petroleum Concession, Pakistan. The seismic lines were provided in SEG-Y format and wireline logs in "LAS" format. The exploratory well Jabo-01 was drilled by Union Texas and it produced gas and condensate, whereas Jabo-03 was drilled by British Petroleum, being a development well, it produced oil and gas [1, 16].

We have interpreted the migrated seismic sections and two key wells. The stepwise procedure adopted in this study is as follows: (i) Well to seismic tie for identification of reflectors using the well data (ii) horizon tracking (iii) correlation of reflectors (iv) fault identification / interpretation using loop

tying (v) time contour mapping (vi) velocity estimation for depth conversion by a suitable polynomial function (vii) horizons mapping in depth (viii) fault seal analysis and (ix) interpretation of the maps by integrating data and results.

The borehole Jabo-01 lies on the seismic line PK86–1200 which are key datasets employed for the calibration purposes in this study. The synthetic seismogram facilitates in comparing the chronological order of stratigraphic horizons gathered from borehole information with the seismic data. The product of seismic wave's velocity (v) and density (ρ) of the formation is called acoustic impedance (z), i.e., $z = \rho v$. Seismic velocity and rock density control the acoustic impedance contrast such as hard rocks horizons exhumed high values of z as compared to the soft rocks. The acoustic impedance function (product of velocity and density [sonic and density log, respectively]) convolved with the reflection coefficient to generate a synthetic seismogram. Fig. 2 illustrated the generation of synthetic seismogram which is prepared by using the digital data of sonic and density logs. By using the values of sonic velocity and density, values of reflection coefficient are calculated, after this an artificial source wavelet is generated; this source wavelet is convolved with the reflection coefficient to generate a synthetic seismogram. Source wavelet has appropriate values of seismic attributes (phase, frequency and amplitude).

Artificial source wavelet and reflection coefficient series are present in the synthetic seismogram. Since the basic difference between both synthetic seismogram and actual seismic reflection is of the source wavelet, so in order to correlate both the synthetic seismogram and seismic section, we change the source wavelet by trial and error process and generate the synthetic that match fully with the actual seismic reflection events. The seismogram is equated to the seismic traces of the nearest seismic section to validate the reflection amplitudes of respective horizons which shows a considerable correlation of horizons (Fig. 2).

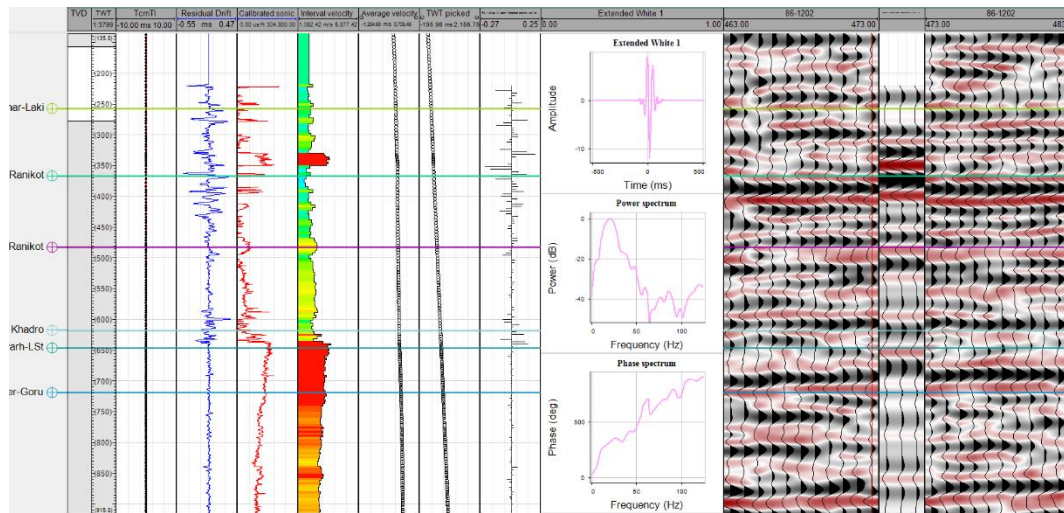


Fig. 2: The systematic process followed to generate the synthetic seismogram for Borehole “Jabo-01” and comparison between synthetic seismogram and the seismic section.

The seismic reflectors (horizons) were marked on PK 86-1200 and subsequently by tying on the other lines of the dataset. All horizons were picked with a careful analysis of reflection configuration, reflection continuity and reflection amplitudes; using auto-tracking mode but in some areas of distortion manual mode was also used. The faults were mapped with the correlation of characteristic reflectors, identification of reflection breaks across the fault plane, variation in dipping pattern along several lines of control. For depth conversion of time maps into depth map, check shot data of Jabo-01 was used. A polynomial function was derived by plotting the depth (y-axis) and time (x-axis). The function was multiplied by the time grid for depth conversion. Though, the Jabo-1 and Jabo-3 only encountered upper sands and not tested the Middle and Basal sands, the depth is corrected for the TLG at these wells by applying the residual grid. Whereas, at Middle and Basal sands the depth is calculated by using the derived function due to the lack of depth control.

3. Results and Discussion

To refine the subsurface model, five horizons were marked, which are abbreviated as: TDCN (Top Deccan/Basalts (Paleocene age)) in the peak (blue), TLG (Top Lower Goru of early Cretaceous) in through (red), TMDS (Top Middle Sand of early Cretaceous) in through (red), TBSL (Top Basal Sand of early Cretaceous) in peak (blue) TCHN (Top Chiltan of middle Jurassic) in peak (blue) whereas the MFL (Main Fault Line) and SFL (Secondary Fault Line) are fault lines.

A special emphasis was given to the TLG reflector since it is proven reservoir of JF and Badin area [16]. Although, the depth of the Jabo-01 is limited to 7304 feet, the deeper horizons were marked using the regional correlation and by character identification on parallel seismic lines PK86-1202 and PK86-1200 (Figs. 3a and 3b). These two dipping seismic profiles cover east-west imaging of the under study region. These seismic lines are showing similar features, the trends of the faulted blocks and their geometries are similar. On the

center of line PK86-1200 a regional fault, MFL dips from NE to SW has a significant throw (50-70 milliseconds approx.); on the western side two other faults dipping toward NE to SW causing deepening towards west; wherein on the eastern side four faults dipping towards NW to SE can be seen on same seismic lines PK 86-1200 and PK 86-1202. The continuity trend of these reflectors indicates a gentle deepening towards East of the JF.

The Seismic profile PK 85-960 interpreted with reference to Jabo-3 located on this dip line. At the eastern side the quality of the data is poor (Fig. 3c). However, the tilted normal fault is marked towards more eastern side of the field. On the western side, a step fault pattern can be seen forming normal faulting structural style (Figs. 3a-c). The regional faults originated from older formations and do not cut through overlying formations indicating that tectonic stresses might be weakened at the time of deposition of relatively younger formations (Upper Goru level) (Figs. 3a-c). This interpretation exercise helped us to define the faults orientation, lateral continuity and penetration of faults in deeper horizons which enhance the structural integrity.

The targeted horizons are seen to be straight on the strike lines PK 85-0935, however, some bulging at the level of TLG, TMDS and TBSL in middle of section (Fig. 3d) corresponds to the horst block uplift and displacements of the up thrown sides (tied in middle of dip lines).

Overall, the geological model of the Jabo Field structure is complex and faulted which require extensive data volume to map the leads and prospects within JF. However, latest published literature [1, 6, 8 and 15] on the structure of study area and nearby areas supports our interpretation and reveal that Jabo structure is located on up thrown side of major tilted fault block (Fig. 3a-c). The Jabo Field is a structurally complex field with numerous splay faults, forming fault compartments within the field. Seismic data quality over the Jabo structure is fair to good which helped to correlate the fault patterns and improved the structural integrity of the

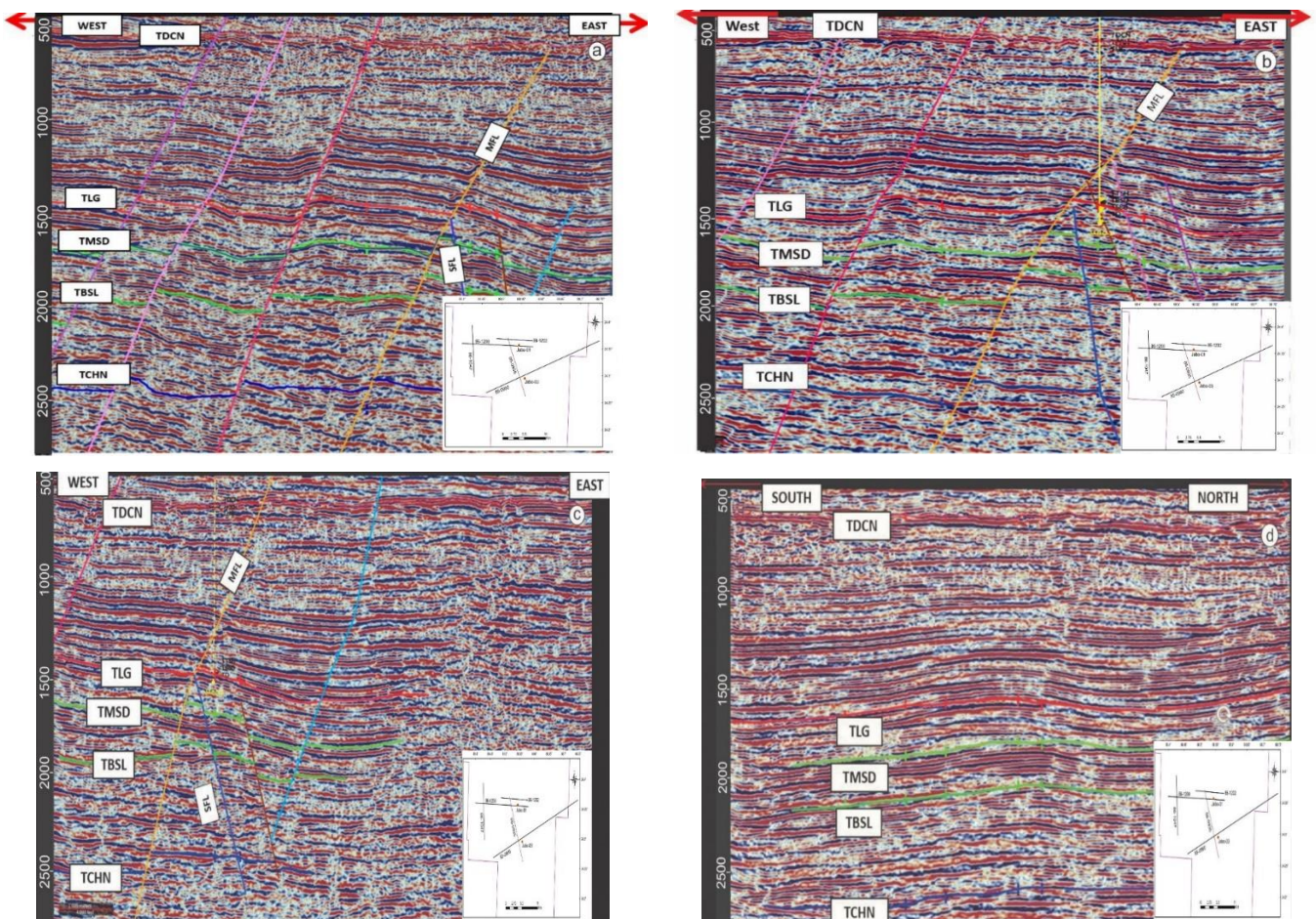


Fig. 3: The interpretation of seismic time sections labeled in milliseconds: (a) seismic line PK86-1202, (b) seismic line PK 86-1200, (c) seismic line PK 85-0960 and (d) seismic line PK 85-0935.

subsurface model. The dominant fault direction in the study area is NNW-SSE. It is postulated that the extensional rifting with some strike slip movement owing to the horst-graben sequence which leads to half grabens and faulted blocks in the study area (Fig. 3a-d). Good seismic response at TLG helped in resolving the structural complexities and separation of the field into the fault blocks.

The isochrone maps vivid the spatial variation of seismic time (seismic two-way-time) for respective geological horizon. The contour maps are generated for better visualization of subsurface and to observe the lateral as well as vertical time changes in the subsurface. Vertical change of time is due to change in density and lithology of the strata, over burden pressure and due to *in-situ* deposition factors [16]. Whereas, the lateral change in time is due to structural disturbance, like folding, faulting and dipping strata. The time contour maps show a picture of lateral subsurface variation in terms of shallow and deeper subsurface geological features.

3.1 Time Structure Maps

The seismic mapping of the two-way-time (TWT) structure at TLG shows that it is a three-way dip closure against the North-West and South-East trending main bounding fault. Closure to the north, south and east of JF is

provided by dip and closure to the west is provided by the MFL. The MFL dips towards west has a throw of around 50-70 milliseconds and SFL dips towards east, characterized with a throw of 20 -30 millisecond (Fig. 4a).

TWT map at TMSD level shows a small structure which is two-way fault bounded and two-way dip bounded. Closure to the north and south is provided by dip, whereas structure is bounded from east and west by fault. The MFL has fault throw of 70-90 millisecond and SFL has fault throw of 25-40 millisecond (Fig. 4b). The vertical relief of this structure is very small, i.e., 40 milliseconds (assuming Structural spill point to be 1680 milliseconds). In the south more in-lines are needed to check the continuity of MFL and possibly higher structural spill point.

Fig. 4c represents the TWT map of a closure structure at TBSL level. The closure to the north and south is provided by the dip of the blocks, from west by MFL (having a throw around 70-120 millisecond) and from east the closure is provided both by SFL and the dip. The throw of SFL is around 30-100 millisecond. However, more data is needed to confirm the closure extent in the south of the study area.

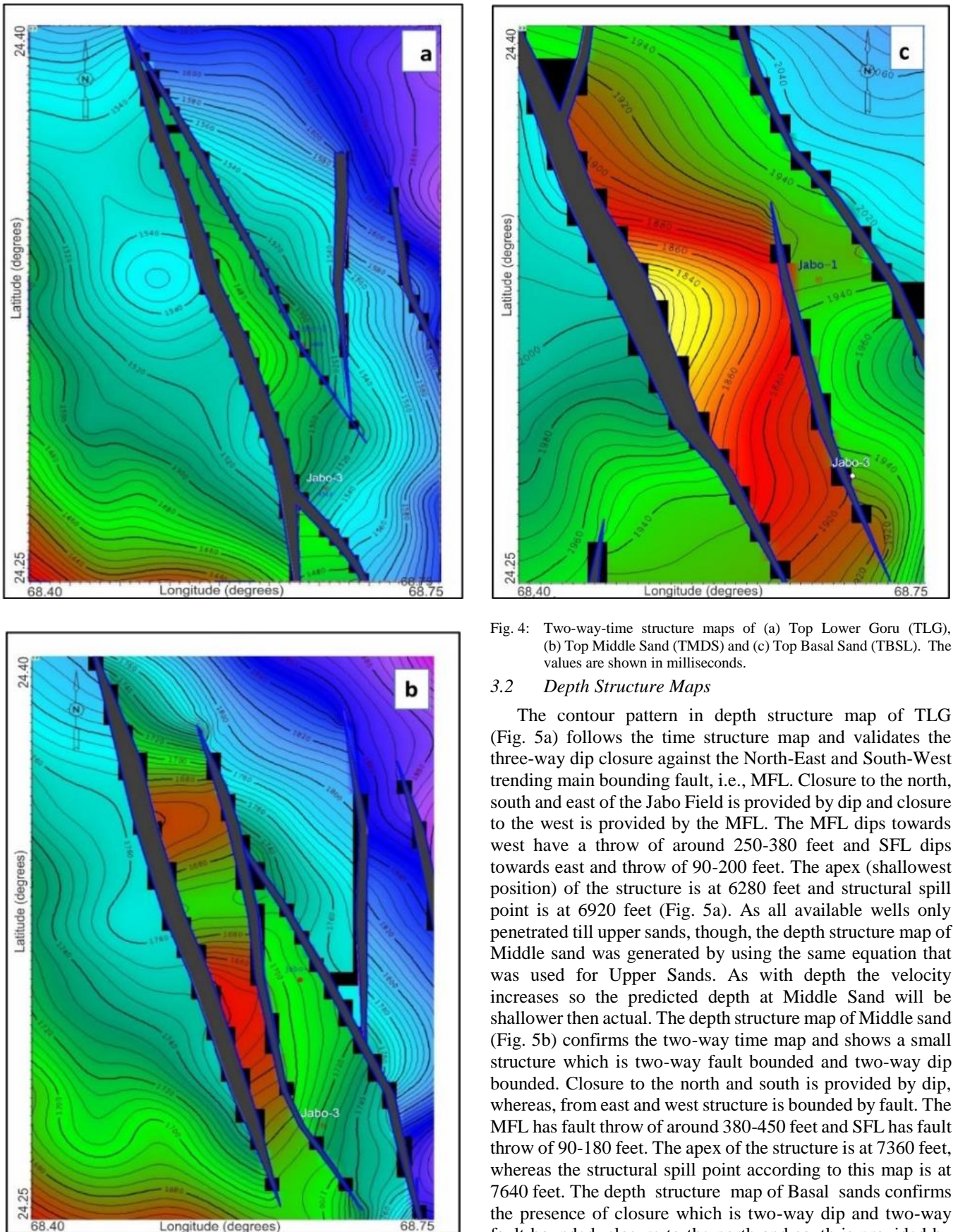


Fig. 4: Two-way-time structure maps of (a) Top Lower Goru (TLG), (b) Top Middle Sand (TMDS) and (c) Top Basal Sand (TBSL). The values are shown in milliseconds.

3.2 Depth Structure Maps

The contour pattern in depth structure map of TLG (Fig. 5a) follows the time structure map and validates the three-way dip closure against the North-East and South-West trending main bounding fault, i.e., MFL. Closure to the north, south and east of the Jabo Field is provided by dip and closure to the west is provided by the MFL. The MFL dips towards west have a throw of around 250-380 feet and SFL dips towards east and throw of 90-200 feet. The apex (shallowest position) of the structure is at 6280 feet and structural spill point is at 6920 feet (Fig. 5a). As all available wells only penetrated till upper sands, though, the depth structure map of Middle sand was generated by using the same equation that was used for Upper Sands. As with depth the velocity increases so the predicted depth at Middle Sand will be shallower than actual. The depth structure map of Middle sand (Fig. 5b) confirms the two-way time map and shows a small structure which is two-way fault bounded and two-way dip bounded. Closure to the north and south is provided by dip, whereas, from east and west structure is bounded by fault. The MFL has fault throw of around 380-450 feet and SFL has fault throw of 90-180 feet. The apex of the structure is at 7360 feet, whereas the structural spill point according to this map is at 7640 feet. The depth structure map of Basal sands confirms the presence of closure which is two-way dip and two-way fault bounded, closure to the north and south is provided by the dip, from west by MFL and from east closure is provided

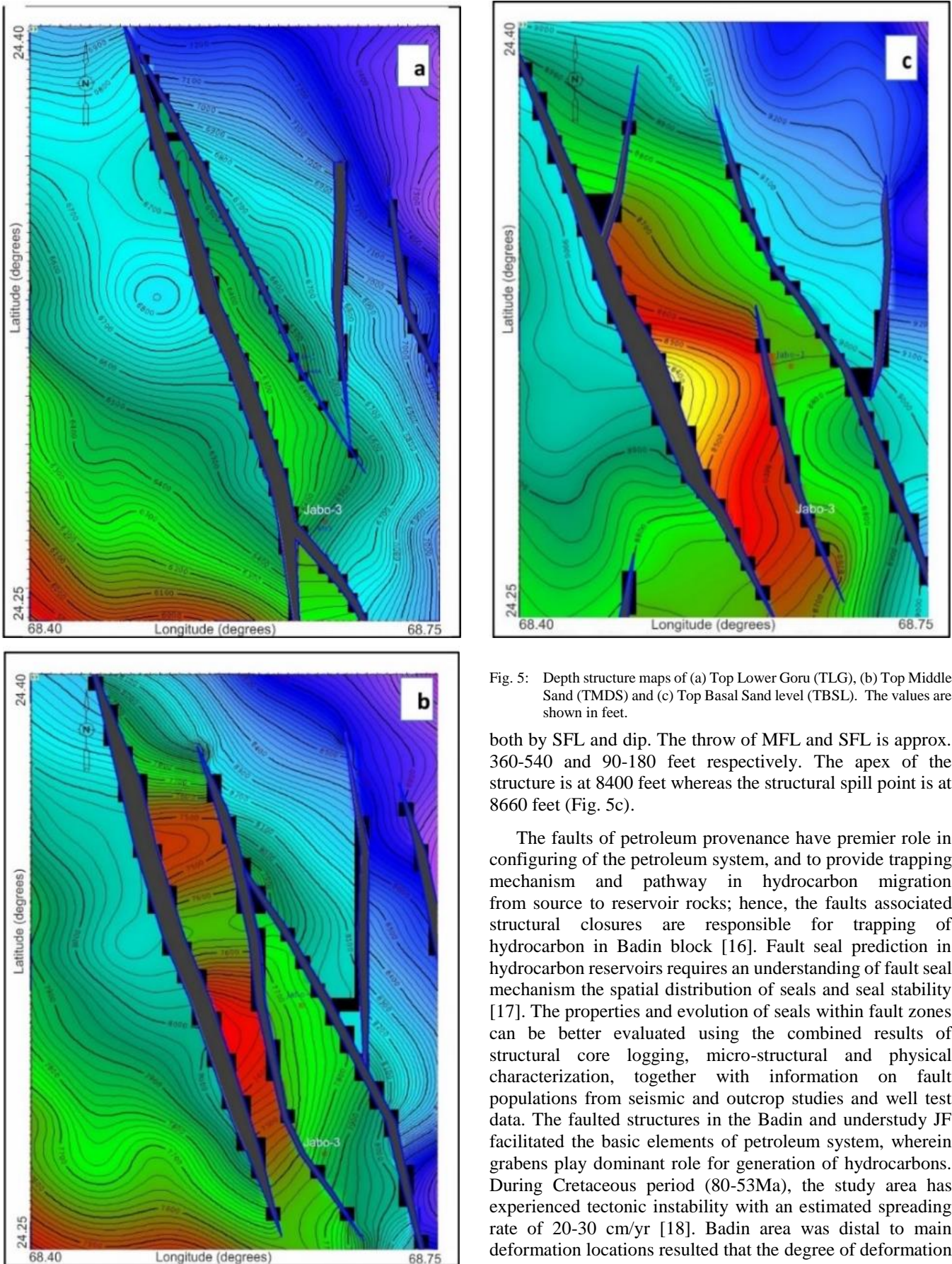


Fig. 5: Depth structure maps of (a) Top Lower Goru (TLG), (b) Top Middle Sand (TMDS) and (c) Top Basal Sand level (TBSL). The values are shown in feet.

both by SFL and dip. The throw of MFL and SFL is approx. 360-540 and 90-180 feet respectively. The apex of the structure is at 8400 feet whereas the structural spill point is at 8660 feet (Fig. 5c).

The faults of petroleum provenance have premier role in configuring of the petroleum system, and to provide trapping mechanism and pathway in hydrocarbon migration from source to reservoir rocks; hence, the faults associated structural closures are responsible for trapping of hydrocarbon in Badin block [16]. Fault seal prediction in hydrocarbon reservoirs requires an understanding of fault seal mechanism the spatial distribution of seals and seal stability [17]. The properties and evolution of seals within fault zones can be better evaluated using the combined results of structural core logging, micro-structural and physical characterization, together with information on fault populations from seismic and outcrop studies and well test data. The faulted structures in the Badin and understudy JF facilitated the basic elements of petroleum system, wherein grabens play dominant role for generation of hydrocarbons. During Cretaceous period (80-53Ma), the study area has experienced tectonic instability with an estimated spreading rate of 20-30 cm/yr [18]. Badin area was distal to main deformation locations resulted that the degree of deformation

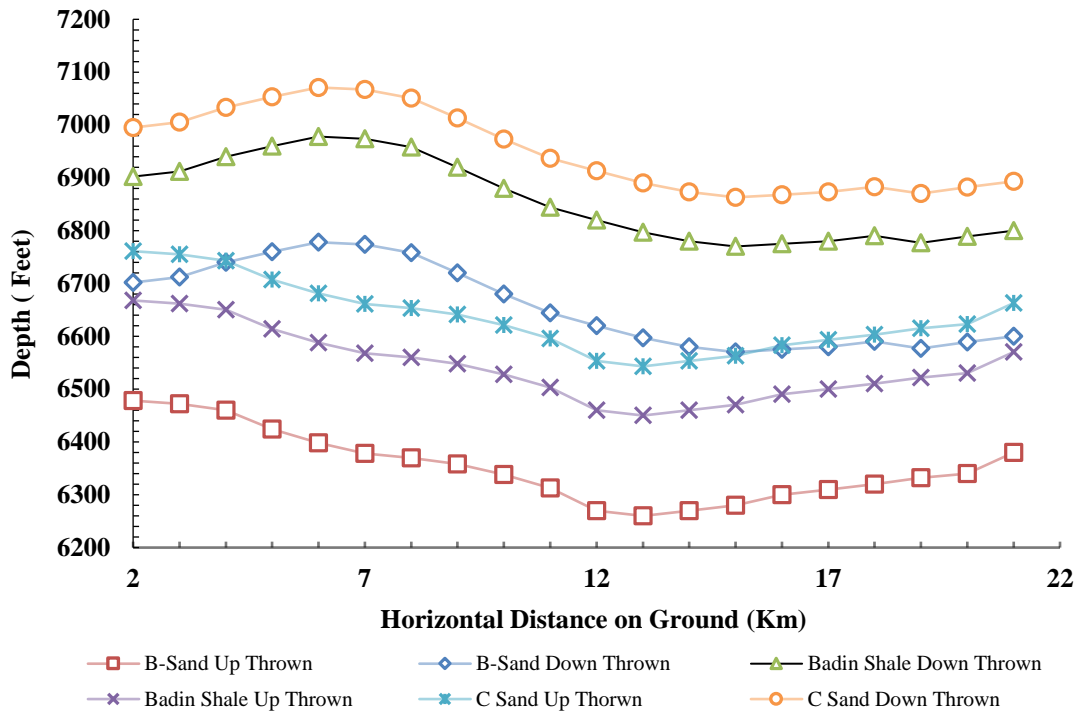


Fig. 6: Allen diagram is presenting the fault seal analysis of lower Goru sequences.

is relatively low and progressively increases from East to West. The seismic reflectors are representing Cretaceous and older layers, which are deformed by a system of faults with normal dip separation. The Cretaceous faults generally strike between N 30° W and N 50° W [19]. The “Allen Diagram” (Fig. 6) shows the lateral juxtaposition of the structural up-thrown with down-thrown, which help to understand the Lateral seal. The up-thrown of B-Sand is juxtaposed against the Upper Goru, i.e., shale so fault is sealing at B-Sand up-thrown. Whereas, at C-Sand up-thrown it is juxtaposed against B-Sand down-thrown which is also; sand, so the fault is leaky at C-Sand up-thrown.

4. Conclusions

Seismic interpretation of the JF is carried out on available 2D seismic data integrated with borehole information of Jabo-01, and Jabo-03. The study is presenting the structural interpretation of the study area, and suggests the presence of tilted normal faulting causing horst and graben structure in JF, which envisaged that the extensional stresses at the southern limb of Sindh monocline. The average throw of the main bounding fault of JF is around 250 – 540 feet. Time and depth structure maps show that structure at TLG level is a one-way fault and three-way dip closure bounded by the north-east and south-west trending MFL. Structure at TMDS level is a two-way fault bounded and through north and south it is bounded by dip. Structural closure at TBSL level is two-way dip and two-way fault bounded; closure to the north and south is provided by the dip, from west by main field fault and from east closure is provided both by SFL and dip. The fault seal analysis confirms that shales of Upper Goru are providing the

lateral seal and vertical seal (Cap rock) to these structural traps of petroleum system in JF.

Acknowledgement

We are thankful to the Directorate General of Petroleum Concession for providing the desired seismic and well data. We express deep sense of gratitude to Prof. Dr. Mubarik Ali, Dr. Ali R. Tabrez, Dr. Iqbal Hajana and Ms. Urooj Shakir for their valuable guidance and suggestions. Authors acknowledge the efforts made by PPL Chair at Earth and Environmental Sciences, Bahria University Karachi Campus for establishing R&D facility at BU Karachi Campus.

References

- [1] S.A. Abbasi, S.H. Solangi, A. Nazeer, S. Asim, W. Habib and I.A. Solangi, “An overview of structural style and hydrocarbon potential of Jabo Field, Southern Sindh Monocline, Southern Indus Basin, Pakistan”, *Sindh Univ. Res. Jour, (Science Series)*, vol. 47, no. 2, pp. 347-354, 2015.
- [2] M.B. Dobrin, “Introduction to geophysical prospecting”, New York, McGrawHill. Book Company, pp. 375, 1976.
- [3] H.N. Al-Sadi, “Seismic exploration”, *J. Can. Soc. Exploration Geophysicists*, vol. 1, pp. 13-43, 1980.
- [4] V.N. Quadri and S.M. Quadri, “Exploration anatomy of success in oil and gas exploration in Pakistan”, *Oil and Gas Journal*, vol. 94, no. 20, pp. 1915-94, 1996.
- [5] N. Ahmed, P. Fink, S. Sturrock, T. Mahmood and M. Ibrahim, “Sequence Stratigraphy as Predictive Tool in Lower Goru Fairway, Lower and Middle Indus Platform, Pakistan”, *Annual Technical Conference*, pp. 85-93, 2004.
- [6] J. Afzal, “Petroleum resource appraisal of Lower Goru Play, Badin Block, Lower Indus Basin, Pakistan”, *Pakistan J. Hydrocarbon Res.*, vol. 8, pp. 12-132, 1996.
- [7] S. Ahmed, “Study on oil and gas distribution in the Badin Block”, *Union Texas Pakistan, Inc., SPE-PAPG, Annual Technical Conference*, pp.137-147, 1999.

- [8] A. Munir, S. Asim, S.A. Bablani and A.A. Asif, "Seismic data interpretation and fault mapping in Badin Area, Sindh, Pakistan", *Sindh University Research Journal (Sci. Series)*, vol. 46, no. 2, pp.133-142, 2014.
- [9] S. Ahmed, S.H. Solangi, M.S.K. Jadoon and A. Nazeer, "Tectonic evolution of structures in Southern Sindh Monocline, Indus Basin, Pakistan formed in multi-extensional tectonic episodes of Indian Plate, Pakistan", *Geodesy and Geodynamics*, vol. 9, no. 5, pp. 456-473, 2018.
- [10] M.J. Khan, M. Ali and M. Khan, "Gamma ray-based facies modelling of lower Goru formation: A case study in Hakeem Daho Well Lower Indus Basin Pakistan", *Bahria Univ. Res. J. Earth Sci.* vol. 2, no. 1, pp. 40-45, 2017.
- [11] M. Ali, M.J. Khan, M. Ali and S. Iftikhar, "Petrophysical analysis of well logs for reservoir evaluation: A case study of "Kadanwari" gas field, middle Indus basin, Pakistan", *Arabian Journal of Geosciences*, vol. 12, no. 6, pp. 215- 224, 2019.
- [12] C.J. Wandrey, B.E. Law and H.A. Shah, "Sembar Goru/Ghazij composite total petroleum system, Indus and Sulaiman-Kirthar Geologic Provinces, Pakistan", *Pakistan and India*. No. 2208-C. 2004.
- [13] S. Ahmed, S.H. Solangi, I.A. Brohi, Q.D. Khokhar and R.A. Lashari "Study of stratigraphy and structural styles in the subsurface of Southern Sindh Monocline, Pakistan: Using seismic and well data", *Sindh Univ. Res. Jour. (Sci. Ser.)*, vol. 46, no. 4, pp. 439-446, 2014.
- [14] A.A. Memon, "The role of cretaceous rifts on the occurrence of oil in Sindh, Monocline, Pakistan", *SPE-PAPG, Annual Technical Conference*, pp. 65-74, 1999.
- [15] M.F. Mahmood, U. Shakir, M.R. Amjad and A. Taimur, "Structural style and hydrocarbon potential evaluation of Badin Block, Lower Indus Basin, Pakistan". *Bahria Univ. Res. Journal of Earth Sci.*, vol. 2, no. 1, pp. 30-34, 2017.
- [16] C. Ebdon, M. Wasimuddin, H.A. Malik and S. Akhter, "Sequence stratigraphy of the B Sand (Upper Sand, Lower Goru Formation) in the Badin area: Implications for development and exploitation", *Annual Technical Conference, Islamabad, Pakistan*, pp. 179-197, 2004.
- [17] F. Campbell, "Fault Criteria", *Geophysics*, vol. 30, no. 6, pp. 976-997, 1965.
- [18] E.A. Gnos, T. Immenhauser and K. Peter, "Late Cretaceous / Early Tertiary Convergence between Indian and Arabian Plates Recorded in Ophiolites and Related Sediments", *Tectonophysics*, 271, pp. 1-19, 1997.
- [19] A. Kemal, A.S.H. Zaman and M. Humayon, "New directions and strategies for accelerating petroleum exploration and production in Pakistan", *Proc. of International Petroleum Seminar, Islamabad, Pakistan, Ministry of Petroleum and Natural Resources*, pp. 16-57, 1991.